Journal of
Renewable Energy Research and Applications (RERA)

Vol. 6, No 1, 2025, 23-33 *DOI: 10.22044/rera.2023.13485.1242*

Design of an On-grid PV System as a Power Backup to Provide a Reliable Electricity Supply

R. Al Hasibi* and B. Hamka

Department of electrical engineering, Universitas Muhammadiyah Yogyakarta, Bantul, Indonesia.

Received Date 16 August 2023; Revised Date 16 November 2023; Accepted Date 17 November 2023
**Corresponding author: r.a.alhasibi@umy.ac.id (R. Al Hasibi)*

Abstract
The implementation of on-grid PV systems was conducted to ensure a continuous supply of electricity. This article discusses implementing an on-grid PV system in a fish farm that requires a continuous electricity supply. Continuous electricity is used to power the aeration system. The aeration system is critical in determining whether or not fish farmers can harvest well. An electric motor drives the water wheel in the aeration system, circulating oxygen in the fishpond. Based on the design, operation, and economic parameters, a comparison is made between the proposed system, namely the PV system, and the current system, namely the grid with a diesel generator as a backup. The nominal discount rate, diesel fuel price, and grid reliability level have all been subjected to sensitivity analysis. The hybrid optimization of multiple energy resources software was used for the study. The results show that the on-grid PV system can continuously provide electricity to meet the demand for fish farming. The proposed system has a net present cost that is 20% lower than the net present cost of the current system. The cost of energy generated by the on-grid PV system is also 27% less than the cost of energy generated by the current system. Changes in fuel prices do not result in changes in net present cost for all levels of grid reliability to produce continuity in electricity supply. The nominal discount rate strongly influences the net present cost, the higher the nominal discount rate, and the lower the resulting net present cost.

Keywords: *Microgrid, On-grid, PV system, Reliability, Sensitivity analysi.*

1. Introduction

Electricity is a form of modern energy required to support all human activities including the economic ones. To support economic activity, electricity must be supplied continuously and with a high degree of reliability. A reliable electricity supply can be obtained with a backup power system, which typically employs a diesel generator with a quick-starting unit [1]. In addition, diesel generators offer financial benefits for both the on-grid [2] and off-grid [3] systems when used as power reserves. This economic advantage is a result of the still-low price of diesel fuel [4]. On the other hand, the use of diesel generators as a backup power source has disadvantages, particularly from an environmental standpoint because diesel generators produce emissions [5]. Nonetheless, there are several methods for reducing diesel generator emissions, including exhaust gas heater [6], hydrogen-oxygen injection [7], and real-time non-surfactant emulsion fuel supply system [8].

The methods for reducing diesel generator emissions still need to be improved to completely eliminate emissions. To completely eliminate emissions, fossil fuel-based electricity generation systems must be replaced with renewable energy-based generation systems [9]. According to previous research, implementing renewable energy can solve not only energy-environmental [10] but also energy-economic [11] and energy-social [12] issues. Renewable energy can generate electricity locally [13] or in remote areas that are not connected to the grid [14]. In fact, some devices like cell phone towers can use renewable energy as a source of electricity [15]. Combining renewable energy with an energy storage system has been shown to be technically and economically viable as a backup electricity source [16].

Solar radiation, used as a source of electrical energy through a photovoltaic (PV) system, is the most widely employed renewable energy source, accounting for 2.1 TW or 62% of total renewable

energy capacity in 2022 [17]. Previous research has addressed using PV as a backup power source for large power systems. If the appropriate control strategy is implemented, PV systems can be utilized as backup power in partial shading [18] and dynamic shading [19] conditions. PV can be combined with other renewable energy sources such as hydro to overcome the flexible load reserve in its operations [20]. In addition, numerous studies have addressed the implementation of PV as an off-grid [21] and on-grid [22] microgrid system. Depending on the electrical load pattern being served, PV can also generate electricity with [23] or without [24] energy storage technology. The use of different tracking systems [25], the reliability of the designed system [26], and highly probabilistic weather [27] all impact the PV system's performance and economy.

Based on the literature review findings, PV has not been utilized extensively as a backup power source, particularly for electrical loads that require a continuous supply of electricity. In addition, a sensitivity analysis must be conducted on the variables that directly impact the implementation of PV as a backup resource, namely fuel price, grid reliability, and nominal discount rate. This article evaluates PV as a backup energy source in a fish farm, where the aeration facility must be supplied with electricity continuously. It has been demonstrated that, in comparison to fish ponds without an aeration system, fish farming with an aeration system increases fish productivity [28]. The challenge that fish farmers experience at the case study area is that the grid's electrical supply is unreliable. Diesel fuel is currently the most viable solution for ensuring the continuity of electricity supply. On the other hand, the government has set targets for reducing emissions in all activity sectors, which are contained in the presidential regulation for 2021. Thus one of the contributions to this presidential decree is the substitution of diesel fuel for renewable energy sources in fish farming.

This article makes the following contributions:

- an analysis of the technical and economic feasibility of the PV system as a backup power source to increase the reliability of electricity supply; and
- a sensitivity analysis of three variables that directly influence the implementation of the PV system as a backup resource.

This article proposes to analyze the PV system as a backup resource to replace the current system, which is a diesel generator-based backup power source. The implementation of the PV system as a backup resource to produce a continuous supply of electricity will be influenced by price variables, namely the price of fuel and electricity. This article's subsequent sections are organized as what follows. Section 2 describes the method used. The second Section describes the software utilized, data of case study, and the mathematical model of the system's constituent parts. In Section 3, results and discussion are presented. In Section 4, conclusions based on the analysis of research results are presented.

2. Materials and methods

This article uses the open-source version of HOMER (Hybrid Optimization of Multiple Energy Resources) Pro [29] to analyze PV systems as a backup power. HOMER has the potential to develop the most cost-effective system configuration. HOMER can be used to (1) combine engineering and economics in a model, (2) allow the users to quickly and efficiently determine least-cost options, (3) simulate real-world performance and deliver a choice of optimized design, and (4) consider geographic-specific criteria and risks such as fuel price changes, load growth, accelerated battery degradation, and changing weather patterns, when designing micro-grid systems or distributed generation systems.

Many studies have been demonstrated that HOMER can explore microgrids comprised of multiple energy supply technologies including green hydrogen, renewable electricity, and heat [30]. HOMER can also be used to conduct comparison studies of various PV panel technologies [31]. Several previous studies have demonstrated HOMER's versatility in analyzing the use of PV systems by sector, specifically in the household [32] and industrial [33] sectors. Furthermore, HOMER can be used to conduct community[34]-based and small-scale [35] analyses of hybrid renewable energy systems (HRES) in order to increase electrification ratios. HOMER can be used for simulation, optimization, and sensitivity analysis [36]. Figure 1 depicts the architecture of the HOMER Pro software.

2.1. Study location

This article presents a case study of a fish farm in Pemalang Regency, Central Java Province, Indonesia (Latitude: 7˚ 20´ South, Longitude: 109˚ 40´ East). This location is situated on the northern coast of Java Island, where the climate is tropical. The highest monthly precipitation is 321 mm^3 in March [37].

2.2. Load profile estimation

There are aeration system pumps, water pumps, and lights among the electrical loads in fish farms. There are two periods in which the electricity load is utilized: the harvest period and the non-harvest period. The aerator fan is turned off during the harvesting period. The electrical load of the fish farm, based on the survey, is detailed in Table 1. Figure 2 and Figure 3 depict the difference in electrical load during and after harvest, respectively. The harvest season occurs three times a year, in January, May, and September.

2.3. Solar resource

The NASA surface meteorology and solar energy database were used to obtain information on solar radiation resources in Pemalang City. Figure 4 depicts solar radiation data. The average solar radiation for one year in Pemalang City is 5.43 kWh/m^2/day with an average clearness index of 0.55 (this fraction indicates that more than half of the solar radiation reaches the earth's surface). The maximum and minimum solar radiation occurred in September (6.6 kWh/m^2/day) and January (4.41 kWh/m^2/day), respectively, as depicted in figure 4. It was determined that the highest production capacity of photovoltaic panels could be anticipated in September.

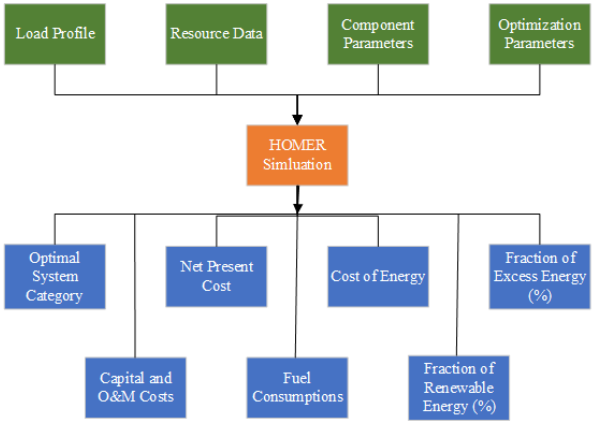

Figure 1. Architecture of HOMER Pro software [38].

Table 1. Electrical load and period of use for each equipment.

Equipment	Electrical power (W)	Quantity	Total power (W)	Period of use
Lamps	30	30	900	06.00 p.m. – 06.00 a.m.
Lamps	15	10	150	06.00 p.m. – 06.00 a.m.
4-inch water pumps	3,000	2	6,000	00.00 a.m. – 23.59 p.m.
6-inch water pumps	7,500	2	15,000	00.00 a.m. – 23.59 p.m.
8-inch water pumps	15,000	1	15,000	00.00 a.m. – 23.59 p.m.
Aerator fan	750	60	45,000	00.00 a.m. – 23.59 p.m.

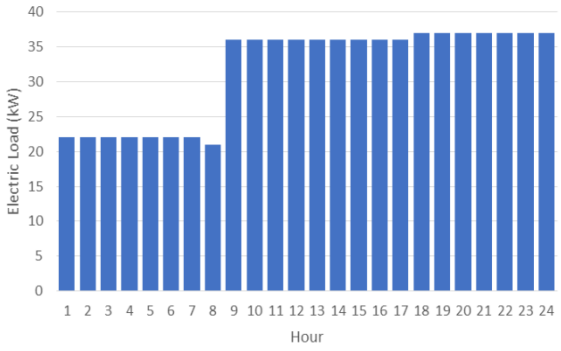

Figure 2. Electric load in harvest periods.

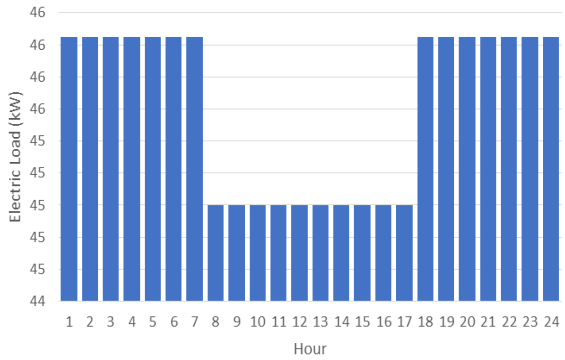

Figure 3. Electric load off-harvest periods.

The production of electricity by PV systems is affected by ambient temperature. In addition to solar radiation reaching the surface of the PV panel, the ambient temperature influences the temperature of the PV cell. Ultimately, the temperature of PV cells will affect the production of electricity. Consequently, the ambient temperature data is one of the parameters used in this article to model the PV system. Figure 5 depicts the temperature in Pemalang City from the same source as solar radiation. The highest and lowest temperatures occur in October (26.06 ˚C) and July (25.38 ˚C).

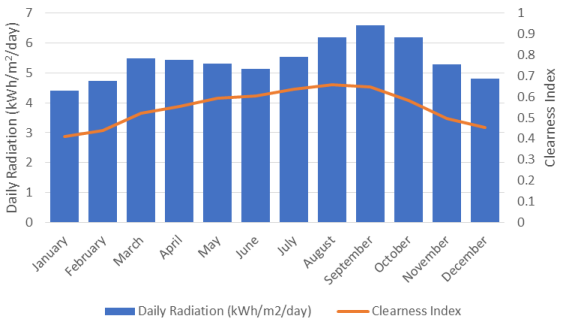

Figure 4. Solar resources of the city of Pemalang, Indoensia.

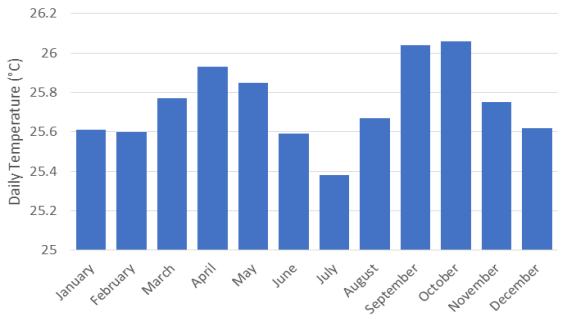

Figure 5. Temperatures of the city of Pemalang, Indoensia.

2.4. Components modeling and parameters

Figure 6 depicts the design of a PV system used as a backup power source. Figure 6 shows a PV module, battery, converter, generator, and grid as system components. The system currently used in fish farming has a grid-based primary power source and a diesel generator for backup power. Each of the system's components is explained in the section that follows.

2.4.1. PV modules

The PV module's power output (P_{pv} in W) can be expressed as [39]:

$$\mathbf{P_{pv} = n_{pv} V_{pv} I_{pv}}$$

where n_{pv} is the number of PV modules, V_{pv} the voltage of PV modules terminals (V), and I_{pv} is the current flow between PV modules terminals (A). Solar radiation and ambient temperature influence the voltage and current generated by each PV panel. Under optimal PV panel operating conditions, the voltage produced by each PV panel is denoted by

$$\mathbf{V_{pv} = V_{max}\left[1 + 0.0539 \times \log\left[\frac{G_T}{G_{st}}\right]\right] + \beta_0(T_A + 0.02 \times G_T - T_{st})}$$

where V_{max} is the maximum voltage of PV panel (V), G_T is solar irradiation on PV panel (W/m^2), G is the standard solar irradiation (1,000 W/m^2), β_0 is the voltage temperature coefficient, T_A is the ambient temperature ($^{\circ}$C), and T_{st} is the standard ambient temperature (25 $^{\circ}$C). When the PV panel is operating optimally, the electric current is stated as:

$$\mathbf{I_{pv} = I_{sc}\left[1 - \left(1 - \frac{I_{max}}{I_{sc}}\right) \times e^{\left(-\frac{V_{max}}{K_2 \times V_{OC}}\right)} \times \left(e^{\left(\frac{V_{max}}{K_2 \times V_{OC}}\right)} - 1\right)\right] + \Delta I}$$

with

$$\mathbf{K_2 = \frac{V_{max}/(V_{OC} - 1)}{\ln\left(1 - \frac{I_{max}}{I_{sc}}\right)}}$$

and

$$\mathbf{\Delta I = \alpha_0 \times \left(\frac{G_T}{G_{st}}\right) \times (T_{pv} - T_{st}) + \left(\frac{G_T}{G_{st}} - 1\right) \times I_{sc}}$$

where V_{OC} is the open-circuit voltage (V), I_{sc} is the short-circuit current (A), and α_0 is the current temperature coefficient.

The PV panels used in this article were selected based on a market survey of the existing PV types and manufacturers. Based on the survey results, the TSM-DE18M PV panel has been chosen. Table 2 displays the technical specifications of these PV panels at standard test condition (STC) and nominal operating cell temperature (NOCT). The per-panel capital cost including shipping fees is USD 251.07. The operating and maintenance cost (OM) of PV panels is USD 14.84 per year.

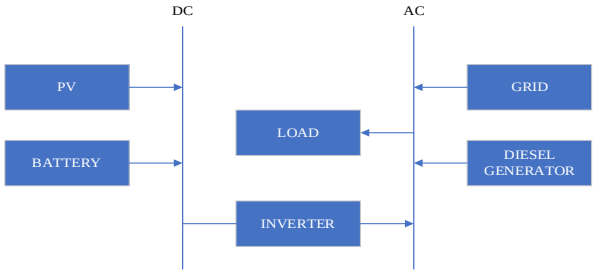

Figure 6. Design of PV system as a back-up power supply.

2.4.2. Batteries

The PV system is supported by energy storage technology as a backup power source. The battery is the energy storage system used in this article. A battery's capacity is its capacity when it is charged and discharged. Battery capacity is a function of time and expressed as:

$$\left.\begin{aligned}\mathbf{C_{chg}(t) = C_{chg}(t-1)(1-\sigma) + \left(P_T(t) - \frac{P_L(t)}{\eta_{conv}}\right) \times \eta_b}\\ \mathbf{C_{dchg}(t) = C_{dchg}(t-1)(1-\sigma) + \left(\frac{P_L(t)}{\eta_{conv}} - P_T(t)\right) \times \eta_b}\end{aligned}\right\}$$

where C_{chg} is the capacity of the battery bank while it is charging and C_{dchg} (W) is the capacity of the battery bank when it is discharged (W). P_T and P_L are the total output power generated by the system (W) and the load demand (W) at the corresponding hour respectively. η_b and η_{conv} are the battery efficiency (%) and the conversion efficiency (%), respectively.

PowerSafe SBS 1500 batteries are utilized in this article. A survey of the types of batteries on the market is also conducted to determine the type of battery used. The cost of one battery including shipping is USD 852.71 with OM cost is USD 46.5 per year. Table 3 lists the technical specifications of this type of battery.

Table 3. Technical specifications of battery [41].

Battery parameters	Value
Nominal voltage	12 V
Nominal capacity	16.7 kWh
Capacity ratio	0.297
Max. discharger current	2300 mAh
Dimension	210 cm x 233 cm x 0,695 cm
Weight	93 kg

2.4.3. Converter

The converter in this article serves as an inverter, converting DC power from the battery to AC power for the electrical load. The inverter used is an ICA Solar SNV-GT1032DM model. The cost of an inverter including shipping is USD 1,984 (capital cost). The annual OM fee for an inverter is USD 98. The inverter's technical parameters are displayed in table 4.

Table 4. Technical specifications of inverter [42].

Inverter parameters	Value
Nominal output power (AC)	10 kW
Nominal AC frequency	50/60 Hz
Maximum efficiency	98%
Power factor	lagging 0.8 – leading 0.8
Dimension (W*L*D)	553 mm x 715 mm x 228 mm
Weight	35 kg

2.4.4. Diesel generator

A diesel generator is currently used as a backup source of electricity. Thus there is no parameter for diesel generators' capital cost. OM costs and fuel prices are the economical parameters of diesel generators. According to a survey conducted at the research site, the OM diesel generator costs USD 200 per year, and fuel costs USD 0.45 per liter. This fuel is priced similarly to subsidized fuel. The capacity of the diesel generator currently used is 50 kW.

2.4.5. Grid

The grid is the primary source of electricity supply in fish farming. The grid parameters used in modeling are the price of grid electricity and the level of grid reliability. The subsidized price of grid electricity is USD 0.96 per kWh. Grid reliability parameters include mean outage frequency (1/yr) and mean repair time (h). The mean outage frequency is the value of the system average interruption frequency index (SAIFI). The mean repair time is the value of the customer average interruption duration index (CAIDI), which is calculated using:

$$\mathbf{CAIDI} = \frac{\mathbf{SAIDI}}{\mathbf{SAIFI}}$$

where SAIDI is system average interruption duration index (h). The distribution network of Pemalang City is part of the distribution network of Central Java Province. According to electricity statistics [43], the value of SAIDI and SAIFI is 7.29 hours and 5.43 times per year, respectively. Thus the average outage rate is 5.43 times per year, and the average repair time is 1.34 hours. HOMER can calculate when a grid outage will occur based on these reliability values. Figure 7 depicts the grid outage calculation results. In figure 7, the green color represents the grid serving the electrical load, and the black color represents a power outage.

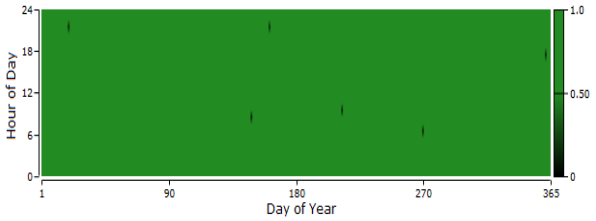

Figure 7. Calculated grid outage.

2.5. Optimization using HOMER

Optimization calculations using HOMER aim to minimize net present cost (NPC). NPC is described as:

$$\mathbf{NPC} = \frac{\mathbf{C_{ann,tot}}}{\mathbf{CRF(d,N)}}$$

where $C_{ann,tot}$ is annualized total cost of the system (USD) and $CRF(d,N)$ is the capital recovery factor that depends on the annual real interest rate. $C_{ann,tot}$ is defined as:

$$\mathbf{C_{ann,tot} = C_{ann,cap} + C_{ann,rep} + C_{ann,O\&M} + C_{ann,fuel} - R_{ann,salv}}$$

where $C_{ann,cap}$, $C_{ann,rep}$, $C_{ann,O\&M}$, $C_{ann,fuel}$, and $R_{ann,salv}$ are annualized capital cost (USD), annualized replacement cost (USD), annualized OM cost (USD), annualized fuel cost (USD), and annualized salvage value of all system component (USD), respectively. Capital recovery factor (CRF) is defined as:

$$\mathbf{CFR} = \frac{\mathbf{d(1+d)^N}}{\mathbf{(1+d)^N - 1}}$$

where d is discount rate (%), and N is the lifetime of the project (year). Discount rate is defined as:

$$\mathbf{d} = \frac{\mathbf{i - f}}{\mathbf{1 + f}}$$

where i and f are nominal interest rate (%) and annual inflation rate (%), respectively. This article considered the discount rate of 5% and the inflation rate of 3%. HOMER calculates the parameter cost of energy (COE) for each system

obtained from optimization in addition to the NPC. The equation is used to calculate COE (USD/kWh) is:

$$\mathbf{COE} = \frac{\mathbf{C_{ann,tot}} - \mathbf{C_{boiler}} \times \mathbf{H_{served}}}{\mathbf{E_{served}}}$$

where C_{boiler} is boiler marginal cost (USD/kWh), H_{served} is total thermal load served (kWh/year), and E_{served} is total electrical load served (kWh/year).

In this article, the constraint function parameters in HOMER are set to maximum annual capacity shortage (%) and minimum renewable energy faction (%). In the simulation and optimization, the maximum annual capacity shortage parameter was set to 0% to simulate a situation where the system could always supply the load on fish farming. The minimum renewable energy fraction parameter is set to 0%, implying that the current system, namely the grid and diesel generator, can be simulated.

Sensitivity analysis can be performed as part of the optimization process using the HOMER software. In this article, the variables utilized in the sensitivity analysis are diesel generator fuel price and grid reliability. In **Error! Reference source not found.**, sensitivity variables are specified in detail. There are two values for the fuel price variable, representing the fuel cost with and without government subsidies. Compared to the existing data, the grid reliability variable represents a state of worse and better reliability. The current situation is represented by sensitivity variables such as a diesel price of 0.45 USD/liter, a grid failure rate of 5.43 per year, and a nominal discount rate of 5%.

3. Result and discussion

The two main topics covered in this section are the optimal system configuration resulting from HOMER simulations and sensitivity analysis. The optimal system configuration is compared to the currently used system. The capacity of each required component is included in the analysis. The three sensitivity variables the price of diesel, the level of grid reliability, and nominal discount rate are used in the sensitivity analysis to compare the economic value of the proposed system.

Table 5. Sensitivity variables and their values.

Sensitivity variable	Value
Diesel price (USD/liter)	0.45; 1.23
Grid failure rate (1/year)	2.5; 3.5; 4.5; 5.43; 6.5; 7.5
Nominal discount rate (%)	5; 6; 7; 8; 9; 10

3.1. Optimal configuration

Compared to other configurations, the optimization calculation results in the on-grid PV system being the most optimal, consisting of PV panels, batteries, inverters, and grids. Table 6 compares an on-grid PV system to the current electricity supply system used in fish farming. The results of this optimization are obtained using the current values of the sensitivity variables, namely the grid failure frequency of 5.43 times per year and the price of diesel fuel at USD 0.45 per liter. The proposed on-grid PV system configuration is shown in the first section of table 6. The following section of Table 6 displays the economic parameters and electricity production.

The proposed system consists of PV panels with a total power of 164 kW, 34 batteries, and a 41.2 kW inverter. This system has an NPC of USD 558,633 and a COE of USD 0.08 per kWh. Compared to the current system, the NPC and COE generated by the on-grid PV system are lower. The on-grid PV system can provide continuous electricity for one year, with 249,747 kWh produced by the PV system and 113,322 kWh purchased from the grid.

Figure 8 depicts the monthly electricity production for the current system in use. As shown in Figure 8, almost all electricity needs are met by the grid, with only 235 kWh generated by diesel generators in one year. Figure 9 depicts the fuel used to generate 235 kWh of electricity per year. The diesel fuel consumption pattern shown in figure 9 represents the diesel generator's function as a backup power source to overcome grid outages (Figure 7). Diesel fuel consumption in one year is 71.1 liters, with an average daily use of 0.20 liters.

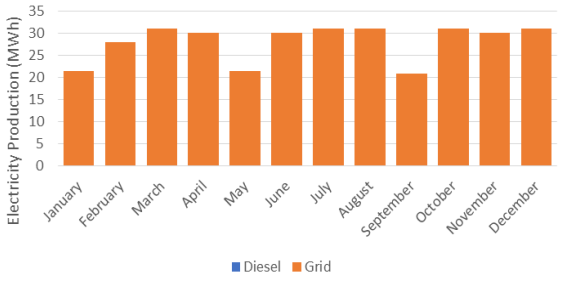

Figure 8. Monthly electricity production by current system.

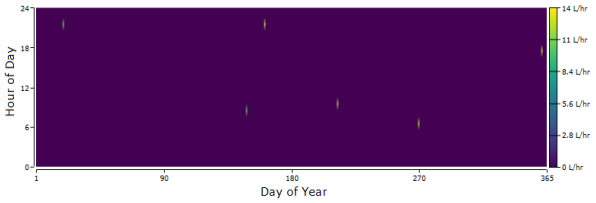

Figure 9. Fuel consumption of diesel generator.

Table 6. Optimization results of proposed and current system.

Item	Component	Unit	Proposed system	Current system
System architecture	PV	kW	164	-
	Battery	Quantity	34	-
	Inverter	kW	41.2	-
	Grid	Yes/No	Yes	Yes
	Diesel Generator	kW	-	50
Cost	COE	USD/kWh	0.08	0.11
	NPC	USD	558,633	693,994
	Fuel	Liter/year	-	33.6
Electricity production	PV system	kWh/year	249,747	-
	Grid purchase	kWh/year	113,322	337,507
	Diesel generator	kWh/year	-	235

Figure 10 shows monthly electricity production of proposed system. The production of electricity from PV systems is highly dependent on solar radiation, as illustrated in Figure 4. The PV system generates more electricity in August, September, and October compared to other months. Due to the occurrence of the rainy season, PV system electricity production decreased in the months following until February. As an on-grid PV system, the electricity load on fish farms still requires monthly grid purchases. Electricity purchased from the grid reached its highest value in February, at 12.53 MWh. Meanwhile, the smallest amount of electricity purchased from the grid was 1.62 MWh in September.

Figure 11 depicts the proposed system's daily operation. As of the previous day, the inverter's output power from the battery was no longer sufficient to serve the load in the early hours of the morning. At this point, the load begins to be served by grid electricity. The load is served by the inverter output during the day once the PV panels have started to convert solar radiation into electricity. A portion of the electricity generated by the PV panels is used to charge the batteries in addition to serving the load during the day. The state of charge (SOC) graph depicts the battery's state of charge, with the SOC value increasing until the afternoon. The PV system can serve the load until 23.00 at night.

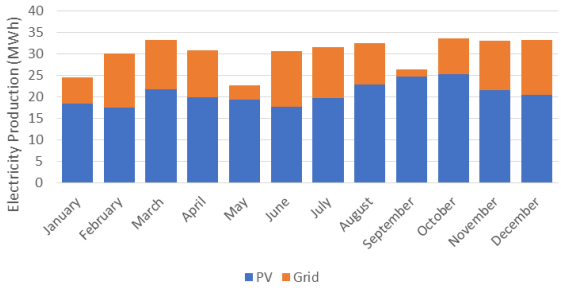

Figure 10. Monthly electricity production by proposed system.

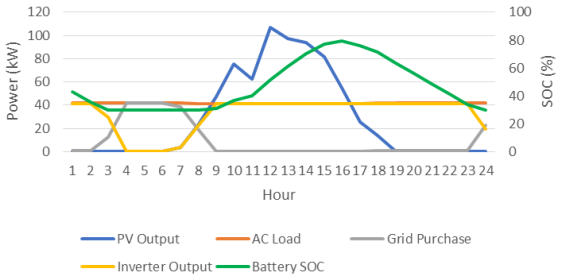

Figure 11. Daily power curve: load, PV panel power, battery SOC, and inverter output power.

Figure 12, Figure 13, and Figure 14 depict operations in the proposed system over the course of a year. Figure 12 depicts the output power of the PV panels. The average power generated by the PV panels is 28.5 kW, despite their rated capacity of 164 kW. As a result, PV panels have a capacity factor of only 17.4%. The average daily electricity production is 684 kWh, with a total annual production of 250 MWh.

The inverter converts the electricity generated by the PV panels to AC power, which is then used to charge the batteries and serve the load. When the PV panels generate electricity, the charging of the batteries begins. Figure 13 shows the SOC value, which indicates the battery charge condition. The SOC value rises throughout the day, peaking in the afternoon. In addition, the SOC value dropped until night. A rise in the SOC value indicates that the batteries are being charged. In contrast, a fall in the SOC value indicates that the electricity in the batteries is being used to power the load via the inverter.

Figure 14 depicts the inverter's output power over a year. With a capacity of 41.2 kW, the average output power produced by the inverters in one year is 25.6 kW, resulting in an overall inverter capacity factor of 62.1%. The inverter's maximum output power is 41.2 kW, equal to the load power to be served. According to Figure 14, the inverter generates output power from morning to night. Meanwhile, the inverter does not produce

electricity in the early morning hours, and the load is served by grid electricity.

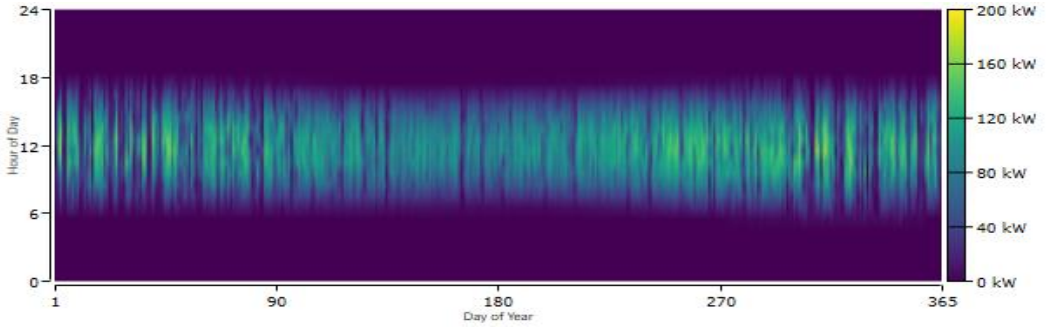

Figure 12. Power output from PV panels.

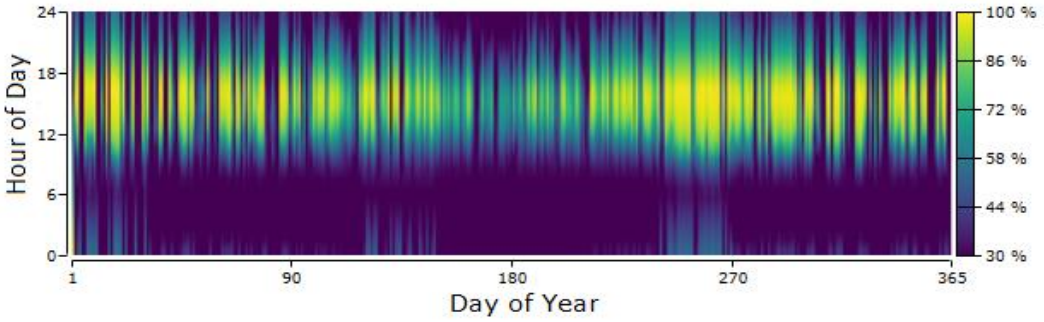

Figure 13. State of charge of the batteries.

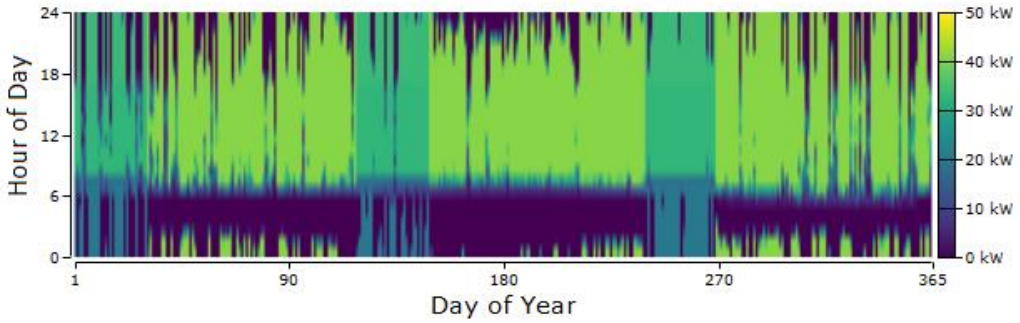

Figure 14. Power output from inverters.

3.2. Sensitivity analysis

Sensitivity analysis is required for decision-makers and investors to decide on renewable energy investment activities. Changes in the sensitivity variables, diesel fuel price, reliability level, and discount rate are used to investigate changes in the resulting optimal system configuration. The economic parameters, namely the NPC, will change if the optimal design of the system is changed. The NPC parameter is a parameter that is frequently used in investment decisions. The discussion in this section focuses on the impact of changes in sensitivity variables on NPC.

Figure 15 depicts the effect of changes in grid reliability and diesel fuel prices on NPC with constant discount rate of 5%. Changes in the grid reliability level result in insignificant changes in the NPC value, as can be seen. Similarly, changes in diesel fuel prices produce two identical curves for diesel prices of 0.45 USD/liter and 1.23 USD/liter. These two similar curves result from setting the maximum annual capacity shortage value to 0% (as discussed in the previous section). Thus electricity demand must be met throughout the year by selecting this value, regardless of grid reliability.

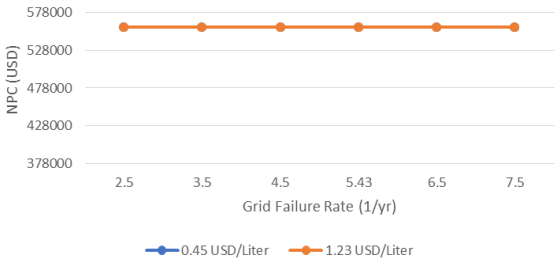

Figure 15. The impact of diesel fuel prices and grid reliability on NPC with discount rate of 5%.

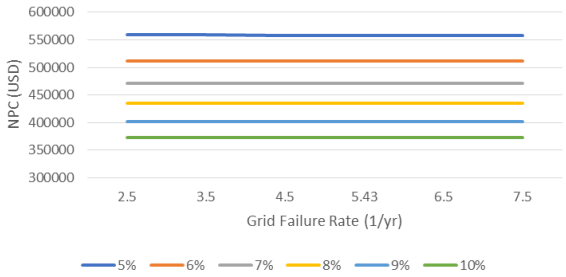

Figure 16. The impact of grid reliability and nominal discount rate on NPC.

Figure 16 depicts the effect of changes in grid reliability level and nominal discount rate on NPC. Figures 15 and 16 show the same results in terms of changes in grid reliability level for NPC, indicating that changes in grid reliability level have no significant effect on NPC. Changes in the nominal discount rate, on the other hand, have a substantial impact on NPC. According to Figure 16, the higher the nominal NPC discount rate, the lower the nominal NPC discount rate. Changes in the NPC value indicate a change in the optimal system configuration, specifically in terms of PV panel capacity, inverter capacity, and the number of battery. Figure 16 depicts the prices of all diesel fuels.

4. Conclusions

A case study of a fish farm that requires a continuous supply of electricity was used to analyze the use of PV systems in providing reliable electricity. In terms of system configuration, economic parameters, and system operation parameters, a comparison of the currently used system, namely the grid with diesel generator backup, and the proposed system, namely the PV system, was performed. According to the optimization results, the proposed system has a lower NPC value than the current system. The proposed system, which consists of PV panels, inverters, and batteries, is more cost effective to implement. Three sensitivity variables, namely diesel fuel price, grid reliability, and nominal discount rate, have been examined for their impact on NPC. Because the designed system must be capable of supplying electricity continuously, changes in diesel fuel prices on the NPC. A shift in grid reliability, on the other hand, has no significant effect on NPC at a constant discount rate. Changes in the nominal discount rate have a considerable impact on NPC. The lower the NPC generated for all levels of grid reliability, the higher the nominal discount rate.

Consideration of uncertain factors such as load changes, price fluctuations, and the unpredictability of renewable energy sources can be incorporated into PV system analysis to ensure a reliable electricity supply. It is possible to develop an optimization model to account for uncertainties in the design of microgrids with renewable energy sources. Using an optimization model with multiple objective functions, cost and environmental parameters can be further analyzed.

5. List of abbreviations

CAIDI	Customer Average Interruption Duration Index
COE	Cost of Energy
HOMER	Hybrid Optimization of Multiple Energy Resources
HRES	Hybrid Renewable Energy System
NOCT	Nominal Operating Cell Temperature
NPC	Net Present Cost
OM	Operating and Maintenance
PV	Photovoltaic
SAIDI	System Average Interruption Duration Index
SAIFI	System Average Interruption Frequency Index
SOC	State of Charge
STC	Standard Test Condition

6. References

[1] Samsun RC, Prawitz M, Tschauder A et al. (2019) An autothermal reforming system for diesel and jet fuel with quick start-up capability. Int J Hydrogen Energy 44:27749–27764. https://doi.org/10.1016/j.ijhydene.2019.08.244.

[2] Rajbongshi R, Borgohain D, and Mahapatra S (2017) Optimization of PV-biomass-diesel and grid base hybrid energy systems for rural electrification by using HOMER. Energy 126:461–474. https://doi.org/10.1016/j.energy.2017.03.056.

[3] Mulenga E, Kabanshi A, Mupeta H et al. (2023) Techno-economic analysis of off-grid PV-Diesel power generation system for rural electrification: A case study of Chilubi district in Zambia. Renew Energy 203:601–611. https://doi.org/10.1016/j.renene.2022.12.112.

[4] Schöne N, Khairallah J, and Heinz B (2022). Model-based techno-economic evaluation of power-to-hydrogen-to-power for the electrification of isolated African off-grid communities. Energy for Sustainable Development 70:592–608. https://doi.org/10.1016/j.esd.2022.08.020.

[5] Sothea K and Kim Oanh NT (2019). Characterization of emissions from diesel backup generators in Cambodia. Atmos Pollut Res 10:345–354. https://doi.org/10.1016/j.apr.2018.09.001.

[6] Ximinis J, Massaguer A, Pujol T, and Massaguer E (2021). Nox emissions reduction analysis in a diesel

Euro VI Heavy Duty vehicle using a thermoelectric generator and an exhaust heater. Fuel 301. https://doi.org/10.1016/j.fuel.2021.121029.

[7] Bari S, Dewar TJ, and Zhang C (2022). Performance and emission characteristics of a diesel engine with on-board produced hydrogen-oxygen injection. Thermal Science and Engineering Progress 32. https://doi.org/10.1016/j.tsep.2022.101317.

[8] Mohd Tamam MQ, Yahya WJ, Ithnin AM et al. (2023). Performance and emission studies of a common rail turbocharged diesel electric generator fueled with emulsifier free water/diesel emulsion. Energy 268. https://doi.org/10.1016/j.energy.2023.126704.

[9] Jiao Y and Månsson D (2023). Greenhouse gas emissions from hybrid energy storage systems in future 100% renewable power systems – A Swedish case based on consequential life cycle assessment. J Energy Storage 57. https://doi.org/10.1016/j.est.2022.106167.

[10] Zhang Z, Mu X, Tu C et al. (2023). Hierarchical network planning of distributed renewable energy in a net-zero energy community. Clean Technol Environ Policy. https://doi.org/10.1007/s10098-022-02461-4.

[11] Ebhota WS and Tabakov PY (2021). Development of domestic technology for sustainable renewable energy in a zero-carbon emission-driven economy. International Journal of Environmental Science and Technology 18:1253–1268. https://doi.org/10.1007/s13762-020-02920-9.

[12] Al Hasibi RA (2021) Multi-objective analysis of sustainable generation expansion planning based on renewable energy potential: A case study of Bali province of Indonesia. International Journal of Sustainable Energy Planning and Management 31:189–210. https://doi.org/10.5278/ijsepm.6474

[13] Razmjoo AA, Davarpanah A, and zargarian A (2019). The Role of Renewable Energy to Achieve Energy Sustainability in Iran. An Economic and Technical Analysis of the Hybrid Power System. Technology and Economics of Smart Grids and Sustainable Energy 4. https://doi.org/10.1007/s40866-019-0063-3.

[14] Anand P, Rizwan M, Bath SK et al. (2022). Optimal Sizing of Hybrid Renewable Energy System for Electricity Production for Remote Areas. Iranian Journal of Science and Technology - Transactions of Electrical Engineering 46:1149–1174. https://doi.org/10.1007/s40998-022-00524-2.

[15] Deevela NR, Kandpal TC, and Singh B (2023). A review of renewable energy based power supply options for telecom towers. Environ Dev Sustain

[16] Li Y, Miao S, Luo X et al. (2020). Dynamic modelling and techno-economic analysis of adiabatic compressed air energy storage for emergency back-up power in supporting microgrid. Appl Energy 261. https://doi.org/10.1016/j.apenergy.2019.114448

[17] IRENA (2023) Renewable capacity statistics 2023.

[18] Verma P, Kaur T, and Kaur R (2021). Power control strategy of PV system for active power reserve under partial shading conditions. International Journal of Electrical Power and Energy Systems 130. https://doi.org/10.1016/j.ijepes.2021.106951.

[19] Verma P and Kaur T (2022). Power reserve control strategy of PV system for active power reserve under dynamic shading patterns. Array 16:. https://doi.org/10.1016/j.array.2022.100250.

[20] Chen Y, Du Q, Wu M et al. (2022). Two-stage optimal scheduling of virtual power plant with wind-photovoltaic-hydro-storage considering flexible load reserve. Energy Reports 8:848–856. https://doi.org/10.1016/j.egyr.2022.05.268.

[21] Aberilla JM, Gallego-Schmid A, Stamford L, and Azapagic A (2020). Design and environmental sustainability assessment of small-scale off-grid energy systems for remote rural communities. Appl Energy 258. https://doi.org/10.1016/j.apenergy.2019.114004.

[22] Vakili S, Schönborn A, and Ölçer AI (2022). Techno-economic feasibility of photovoltaic, wind and hybrid electrification systems for stand-alone and grid-connected shipyard electrification in Italy. J Clean Prod 366. https://doi.org/10.1016/j.jclepro.2022.132945.

[23] Zhu J hong, Ren H, Gu J et al. (2023). Economic dispatching of Wind/ photovoltaic/ storage considering load supply reliability and maximize capacity utilization. International Journal of Electrical Power and Energy Systems 147. https://doi.org/10.1016/j.ijepes.2022.108874.

[24] Kallel R and Boukettaya G (2022). An energy cooperative system concept of DC grid distribution and PV system for supplying multiple regional AC smart grid connected houses. Journal of Building Engineering 56. https://doi.org/10.1016/j.jobe.2022.104737

[25] Praliyev N, Zhunis K, Kalel Y et al. (2020). Impact of both one-and two-axis solar tracking on the techno-economic viability of on-grid PV systems: Case of the burnoye-1 power plant, Kazakhstan. International Journal of Sustainable Energy Planning and Management 29:79–90. https://doi.org/10.5278/ijsepm.3665.

[26] Paliwal P (2020) Reliability constrained planning and sensitivity analysis for solar-wind-battery based isolated power system. International Journal of Sustainable Energy Planning and Management 29:109–126. https://doi.org/10.5278/ijsepm.4599.

[27] Meschede H, Hesselbach J, Child M, and Breyer C (2019). On the impact of probabilistic weather data on the economically optimal design of renewable energy systems – A case study of la gomera island.

International Journal of Sustainable Energy Planning and Management 23:15–26. https://doi.org/10.5278/ijsepm.3142.

[28] Mengistu SB, Mulder HA, Benzie JAH et al. (2020). Genotype by environment interaction between aerated and non-aerated ponds and the impact of aeration on genetic parameters in Nile tilapia (Oreochromis niloticus). Aquaculture 529. https://doi.org/10.1016/j.aquaculture.2020.735704.

[29] UL Solutions (2023) HOMER Energy—the microgrid software. https://www.homerenergy.com/products/pro/index.html. Accessed 31 May 2023

[30] Di Micco S, Romano F, Jannelli E et al. (2023). Techno-economic analysis of a multi-energy system for the co-production of green hydrogen, renewable electricity and heat. Int J Hydrogen Energy. https://doi.org/10.1016/j.ijhydene.2023.04.269.

[31] Irshad AS, Ludin GA, Masrur H et al. (2023). Optimization of grid-photovoltaic and battery hybrid system with most technically efficient PV technology after the performance analysis. Renew Energy. https://doi.org/10.1016/j.renene.2023.03.062.

[32] Enongene KE, Abanda FH, Otene IJJ et al. (2019). The potential of solar photovoltaic systems for residential homes in Lagos city of Nigeria. J Environ Manage 244:247–256. https://doi.org/10.1016/j.jenvman.2019.04.039.

[33] Azerefegn TM, Bhandari R, and Ramayya AV (2020). Techno-economic analysis of grid-integrated PV/wind systems for electricity reliability enhancement in Ethiopian industrial park. Sustain Cities Soc 53. https://doi.org/10.1016/j.scs.2019.101915.

[34] Benti NE, Mekonnen YS, and Asfaw AA (2023). Combining green energy technologies to electrify rural community of Wollega, Western Ethiopia. Sci Afr 19. https://doi.org/10.1016/j.sciaf.2022.e01467.

[35] Fosso Tajouo G, Tiam Kapen P, and Djanna Koffi FL (2023). Techno-economic investigation of an environmentally friendly small-scale solar tracker-based PV/wind/Battery hybrid system for off-grid rural electrification in the mount bamboutos, Cameroon. Energy Strategy Reviews 48. https://doi.org/10.1016/j.esr.2023.101107.

[36] Demirci A, Akar O, and Ozturk Z (2022). Technical-environmental-economic evaluation of biomass-based hybrid power system with energy storage for rural electrification. Renew Energy 195:1202–1217. https://doi.org/10.1016/j.renene.2022.06.097.

[37] Statistics Indonesia (2023) Pemalang Regency in Figures 2023.

[38] Razmjoo A, Shirmohammadi R, Davarpanah A et al. (2019). Stand-alone hybrid energy systems for remote area power generation. Energy Reports 5:231–241. https://doi.org/10.1016/j.egyr.2019.01.010.

[39] Al-Sharafi A, Sahin AZ, Ayar T, and Yilbas BS (2017). Techno-economic analysis and optimization of solar and wind energy systems for power generation and hydrogen production in Saudi Arabia. Renewable and Sustainable Energy Reviews 69:33–49.

[40] Trina Solar (2023) Mono Multi Solutions THE BACKSHEET MONOCRYSTALLINE MODULE. https://pages.trinasolar.com/rs/567-KJK-096/images/DE18m%20Datasheet%20update.pdf. Accessed 26 Jun 2023.

[41] EnerSys PowerSafe SBS Battery. https://www.enersys.com/en/products/batteries/powersafe/powersafe-ms500/. Accessed 26 Jun 2023.

[42] ICA Solar String Inverter SNV-GT1032DM.

[43] PLN (2022) Electricity Statistics. https://web.pln.co.id/statics/uploads/2023/05/Statistik-PLN-2022-Final-2.pdf. Accessed 27 Jun 2023.